

Alpha structure of ^{16}O at high excitation energies by $^{3}\text{He} + ^{13}\text{C}$ nuclear reactions

Luigi Redigolo^{1,2,*}, Ivano Lombardo^{1,3}, Daniele Dell'Aquila^{2,4}, Mariano Vigilante^{2,4}, Mualla Ayketin⁵, Lucia Baldesi^{6,7}, Sandro Barlini^{6,7}, Alberto Camaiani^{6,7}, Giovanni Casini^{6,7}, Caterina Ciampi^{6,7}, Daniela Fabris⁸, Magda Cicerchia^{5,9}, Catalin Frosin^{6,7}, Fabiana Gramegna⁹, Tommaso Marchi⁹, Antonio Ordine^{6,7}, Pietro Ottanelli^{6,7}, Gabriele Pasquali^{6,7}, Silvia Piantelli⁷, Marco Russo^{1,2}, Andrea Stefanini^{6,7}, Simone Valdrè⁷, and Giuseppe Verde²

¹Dipartimento di Fisica e Astronomia "Ettore Majorana", Università di Catania, Via S. Sofia, Catania, 95123, Italy

²Istituto Nazionale di Fisica Nucleare, Sezione di Catania, Via S. Sofia, Catania, 95123, Italy

³Dipartimento di Fisica "E. Pancini", University of Naples Federico II, Via Cintia, Naples, 80126, Italy

⁴Istituto Nazionale di Fisica Nucleare, Sezione di Napoli, Via Cintia, Naples, 80126, Italy

⁵Dipartimento di Fisica e Astronomia, University of Padova, Via Marzolo, Padua, 30020, Italy

⁶Dipartimento di Fisica, University of Firenze, Via G. Sansone, Sesto Fiorentino (FI), 50019, Italy

⁷Istituto Nazionale di Fisica Nucleare, Sezione di Firenze, Via G. Sansone, Sesto Fiorentino (FI), 50019, Italy

⁸Istituto Nazionale di Fisica Nucleare, Sezione di Padova, Via Marzolo, Padua, 30020, Italy

⁹Istituto Nazionale di Fisica Nucleare, Lab. Nazionali di Legnaro, Via dell'Università, Legnaro (PD), 35020, Italy

Abstract. This work investigates high energy states in the self-conjugate ^{16}O nucleus, through the analysis of $^{13}\text{C}(^{3}\text{He},\alpha)^{12}\text{C}$ reactions in the 1.4 - 2.2 MeV bombarding energy range. The cross-section of the decay channel in which an α particle is emitted in coincidence with a ^{12}C residual nucleus in the Hoyle state, leading to four α particles in the final channel, has been measured thanks to a low-threshold and high-resolution array. The occurrence of two low-spin resonant states is highlighted by the analysis of angular distributions, with $J^\pi = 2^+$ and 3^- , at respective energies of ≈ 24.1 and 24.5 MeV. In this energy window, the observed branching ratios for the transition involving the emission of the Hoyle state appear to be way larger than calculations based on the barrier penetration alone, pointing out to the possible occurrence of largely clustered high-energy states in ^{16}O .

1 Introduction

One of the most important topics in nuclear physics, as today, is the study of the cluster structures of self-conjugated nuclei [1–4], such as ^{12}C , ^{16}O , ^{20}Ne , ^{24}Mg and the interplay that may arise between shell and clustering effects in light nuclei. Pointing out these phenomena may help unveil and understand in a deeper way the behaviour of long-range correlations in nuclear forces [5]. Although similar assumptions and theories can be supplemented by a large amount of experimental campaigns [6–10] and theoretical works [11, 12] for the ^{12}C (both in the ground and the Hoyle states [13, 14]), the same is not true for the ^{16}O nucleus.

Indeed, the ^{16}O spectroscopy is particularly important: this nucleus, in fact, is both doubly magic and self-conjugated, with the lowest separation threshold being that for the $^{12}\text{C} + \alpha$ particle decay. Tetrahedral structures (or more exotic ones such as squares or kites) have been predicted for the ground or excited states within various theoretical frameworks [15–17]. Some recent works focused on the hunt of Hoyle-analogue states at energies approaching the 4α particles disintegration threshold, with a gas or linear chain structure [18], but did not succeed in giving

ing clear answers yet. The picture is even less clear at higher excitation energies ($E_x > 19$ MeV), where several high-spin states have been predicted by theoretical models, but only some correspondences have been, up to date, found with experimental data [15, 19]. The investigation of the nature of low-spin states in ^{16}O at very high energies is even more difficult, because of the still sparse spectroscopic information nowadays available [20]. The existence of various 0^+ states with pronounced α structures in this energy range was predicted several decades ago by the *quartet model* [21], but still lacks of enough correspondences in experimental data [22].

In this context, the study of reaction channels such as the $^{3}\text{He} + ^{13}\text{C} \rightarrow ^4\text{He} + ^{12}\text{C}$ at energies well lower than the Coulomb Barrier (≈ 2.8 MeV) can be extremely useful, thanks to the coupling of the large $^{3}\text{He} + ^{13}\text{C}$ separation energy in ^{16}O and the low bombarding energies, which leads to the selective population of states of the ^{16}O compound nucleus with high E_x and low-spin. Furthermore, another important feature is the possibility to study, with a straightforward two-body kinematic process, the *golden channel* linked to the α -transition which leads to the residual ^{12}C in the Hoyle state, crucial to highlight the presence of very pronounced cluster structures in ^{16}O .

*e-mail: luigi.redigolo@ct.infn.it

In the last years, sophisticated four-particles correlation experiments were indeed performed [23–25] to reconstruct the oxygen decay in the $\alpha + {}^{12}\text{C}$ (Hoyle) four alpha channel at high excitation energies; however, in Ref. [23] the highest excitation energy reached was $E_x \approx 22$ MeV, while in Ref. [25] no clear structures in the $E_x \approx 18 - 27$ MeV region were observed.

On the experimental side, in the energy region below the Coulomb Barrier, very few experimental data are available on ${}^3\text{He} + {}^{13}\text{C}$ reactions. Some experimental cross section data were reported for the ${}^{13}\text{C}({}^3\text{He}, \alpha_{0,1}){}^{12}\text{C}$ channels. Ref. [26] reports data on the $\alpha_{0,1,2}$ channels, but only at over-barrier energies, while one of the very rare works regarding under-barrier data for the Hoyle (α_2) channel is discussed in Ref. [27], but not without showing sizeable difficulties when trying to measure the α_2 transition with a single-stage detector, which ends up being overwhelmed by peaks coming from contaminant reactions.

To seek solutions on these issues, in this work, the ${}^{13}\text{C}({}^3\text{He}, \alpha){}^{12}\text{C}$ reaction channels were studied thanks to a solid-state hodoscope array with very low identification threshold, large angular coverage and high energy resolution. Through the measurement and the analysis of the integrated cross-section data, it was possible to reconstruct the ${}^{16}\text{O}$ excited states decay branching ratio in the channels leading to the *ground* and to the *Hoyle* states of ${}^{12}\text{C}$. The presence of the anomalous values for this branching ratio is likely linked to the appearance of cluster effects at high excitation energies in the ${}^{16}\text{O}$ parent nucleus.

2 Experimental setup

The HELICA Experiment was performed at the INFN-LNL (Laboratori Nazionali di Legnaro, Italy) AN-2000 *Van de Graaf* accelerator, using singly-charged Helium-3 beams with energies ranging from $\approx 1.4 - 2.2$ MeV, with 20 keV steps on average, intensities from a minimum of ≈ 70 to a maximum of ≈ 90 nA, measured through a Faraday cup. The beam had a very narrow spot size (≈ 2 mm in diameter), and a resolution better than 1 keV. The target was a self-supporting foil of ${}^{13}\text{C}$, enriched a 99% level and with a thickness of $29 \mu\text{g}/\text{cm}^2$. A sketch of the geometries of the detection array is reported in Figure 1: as shown, it is composed by four OSCAR modules [28–31] arranged symmetrically around the target. A single OSCAR module is a solid state hodoscope, based on two detection stages (a Single Sided Silicon Strip Detector, SSSSD, of $20 \mu\text{m}$ of thickness, and a second plane of sixteen $500 \mu\text{m}$ thick silicon pads, with nominal active areas of 1 cm^2), and identified, as in 1, by four different colours, *Verde*, *Blu*, *Rosso* e *Nero*. In this setup, OSCAR *Verde* and OSCAR *Blu* covered the detection in the forward hemisphere, while OSCAR *Rosso* and OSCAR *Nero* were dedicated to the detection in the backward hemisphere; in both the forward and backward regions, one of the two detectors (OSCAR *Verde* and OSCAR *Rosso*) was mounted without the first SSSSD stage, that was replaced by a thick aluminum absorber to detect high-energy protons emitted in the ${}^3\text{He} + {}^{13}\text{C}$ reactions. As shown in the figure, to avoid the impinging of large flux of elastically scattered particles into the

detectors, the OSCAR *Nero* and *Blu* units were preceded by a thin *mylar* foil. The detection solid angles were estimated, with a resolution of $\approx 3\%$, through precise Monte Carlo simulations, bench-marked with runs of Rutherford scattering of protons on gold and ${}^{12}\text{C}$ targets, while the energy calibration of detectors was made through a mixed nuclide α -source and elastic scattering reference points.

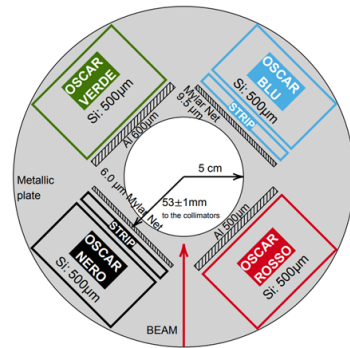


Figure 1. A schematic representation of the detection array composed by the four OSCAR Units.

Thanks to the low threshold, high coverage and high resolution array, it was possible to obtain, for Helium isotopes, an average identification threshold of ≈ 6 MeV and an energy resolution of ≈ 60 keV. The front-end electronics was cooled with liquid circulation in vacuum, and the whole scattering chamber, encapsulating the very compact set-up, was kept at a residual pressure of around 10^{-6} mbar.

Particles identification was unambiguously confirmed, in mass and charge, thanks to the combination of $\Delta E - E$ matrices (which allow to identify separated bumps related to $({}^3\text{He}, p)$ and $({}^3\text{He}, d)$ reactions and to the ${}^{12}\text{C} + \alpha_i$ channels) and the analysis of the kinematic loci ($E_\alpha(\theta)$) of the well identified α particles. The loci were perfectly reproduced by kinematic calculations for the 0, 4.44, 7.65 and 9.63 MeV excited states in ${}^{12}\text{C}$, populated by the ${}^{13}\text{C}({}^3\text{He}, \alpha_i){}^{12}\text{C}$ reactions. This clear separation, and the excellent agreement between experimental data and calculation, are valid in both the backward and forward hemisphere, and in the whole explored beam energy range.

3 Analysis of the angular distributions and integrated cross sections

The count yields for the $\alpha_{0,1,2}$ particle channels were transformed into absolute Differential Cross Sections (DCS) by taking into account all the following parameters: the areal density of the target, the solid angle subtended by each given pseudo-telescope, the integrated current, and the correction for the dead time, yielding an estimated systematic uncertainty lower than 8%. The absolute DCS values extracted in this work for the $\alpha_{0,1}$ channels are in reasonable agreement with data reported from previous literature works [27, 32–34]. The α_0 channel angular distributions were then decomposed in Legendre polynomials, truncated to the 4th order; this assumption is justified

by the low energy of the beam, which in this well under-barrier framework, would exhibit dominant character from lower ℓ_i values. Angular distributions (ADs) in the whole energy and angular domains are well reproduced by the fit based on the mentioned Legendre polynomials.

The analysis was made easier by the zero channel-spin of the outgoing α_0 channel, which only allows the population of *natural parity* states in the ^{16}O compound nucleus (as in [35–37]); however, the draw of the J^π values of these states from the analysis of the angular distributions is not as direct as in other cases with zero channel-spin in both the entrance and the exit channels, or of incoming and outgoing reaction channels with the same intrinsic parity [38]. In the case of the reaction analyzed in this work, the J^π of the projectile and target nuclei are, respectively, $\frac{1}{2}^+$ and $\frac{1}{2}^-$: their combination would give an entrance channel spin of $S_i = 0, 1$ with a negative intrinsic parity.

Still, despite the complications given by the present case, various theorems valid for compound nucleus reactions [39, 40], allow to consistently apply some selection rules to the analysis of the Legendre polynomial expansion of the experimental ADs, due to angular momentum and parity conservation [41, 42] restrictions. Thanks to this, the observation of the behaviour of the B_i coefficients is used to forecast J^π assignments for the ^{16}O excited states. By analyzing the trends of the $B_i(E_x)$ terms for the α_0 , it is possible to see a broad increment in the B_2 term, in the region between $E_{cm} \approx 1.2 - 1.6$ MeV, which can be seen in a clearer way when a normalization to the zero-order coefficient ($\frac{B_2}{B_0}$) is applied. The observed bump suggests the presence of an isoscalar state in the ^{16}O compound nucleus at $E_x \approx 24.1$ MeV, with an estimated width of $\Gamma \approx 260$ keV. In the same energy region, the B_4 term, which is the subsequent *even* term of the series, shows a flat behaviour, way smaller than the B_2 term, and given by the presence of the low-energy tail of a higher energy lying state. Asserting the dominance of the B_2 term is important because it would restrict at least one of the ℓ_i , J and ℓ_f terms to be equal to 1, while the remaining ones must be > 1 . Other considerations on the coupling with the channel spin and the rules on parity conservation allow to restrict the J^π assignments of the 24.1 MeV state to two values: 1^- and 2^+ .

At variance, at higher energies ($E_{cm} > 1.6$ MeV), it is possible to observe a constant increment of the B_4 term, which morphs into a bump at $E_{cm} \approx 1.8$ MeV, suggesting the appearance of another isoscalar state around $E_x \approx 24.5$ MeV with a width of $\Gamma \approx 290$ keV; however, these estimates could be unfortunately biased by the finite data range, close to the maximum energy of the beam delivered by the accelerator. As in the previous case, based on Refs. [39, 41, 42], a $J^\pi = 3^-$ assignment would be favored by the dominance of the B_4 term and the $\ell_{in} \leq 2$ restriction given by the low energy of the beam.

To eliminate the ambiguity on the J^π assignment for the 24.1 MeV state, it is possible to look at the behaviour of the *odd* coefficients, especially the B_3 term, which shows a broad bump at intermediate energies, between those of the two investigated resonances: this points out

the existence of interference effects between neighboring states of *opposite* parities. This would, therefore, force the $J^\pi = 2^+$ assignment for the 24.1 MeV state.

On the other hand, the same Legendre Polynomial analysis is more complicated for the α_1 channel ADs, since the final channel has non-vanishing channel-spin too, with the residual ^{12}C nucleus being no more in its ground state. However, the behaviour of the B_i distributions is coherent with expectations coming from the J^π values suggested in the α_0 case. All of these features can help to assert the dominance of the compound nucleus mechanism for the $^{13}\text{C}(^3\text{He},\alpha_i)^{12}\text{C}$ reactions over direct processes, in the investigated energy range, as already reported at slightly higher energies by [27]. By comparison with previous literature data, as listed in [20], it is possible to underline a correspondence between the states here reported and those already listed for $^3\text{He} + ^{13}\text{C}$ systems at 24.1 and 24.4 MeV, with respective widths of 450 and 250 keV, but without firm J^π assignment. Furthermore, it is also possible that the higher-energy state observed in this work could correspond to an isoscalar state previously seen in the ^{16}O neutron decay, at 24.36 ± 0.07 MeV, for which the J^π was only tentatively assigned as 2^+ or 3^- [20].

From the Legendre polynomial analysis of the ADs is possible to extract the integrated cross sections (ICS) for all the explored reaction channels. The trends of the ICS for the $\alpha_{0,1,2}$ channels have similar shapes in the energy range here studied; however, the ICS for the α_1 channel is about one order of magnitude larger than those of the α_0 and α_2 channels (which are, in turn, comparable), since it is not hindered by the conservation rules on natural parity states and is enhanced by the statistical weight of the $J = 2$ of the 4.44 Mev state in ^{12}C . In the case of the α_2 channel, the particles emitted in the backward hemisphere can be partly cut out by identification threshold effects at some bombarding energies, while no biases were observed in the forward hemisphere; however, the shape of the α_2 ADs is quite similar in the whole explored bombarding energy range. An *average correction factor* was thus estimated to evaluate the effect of asymmetries between the two hemispheres in the reconstruction of the ICS; it is worth noting that similar ADs asymmetries were found in [27] for two ADs at $E_{lab} < 2$ MeV.

4 Estimation of the Branching Ratio of the Hoyle to the Ground state transitions

The de-excitation of ^{16}O states at excitation energies greater than ≈ 15 MeV may happen through the emission of α particles and a residual ^{12}C nucleus which can be left in its ground state or in some of the low-lying excited states. In the compound nucleus scenario here dominant, the ratio of the cross section of the two channels ($\frac{\sigma_{\alpha_2}}{\sigma_{\alpha_0}}$) is related to the branching ratio (BR) of the partial widths $BR = \frac{\Gamma_{\alpha_2}}{\Gamma_{\alpha_0}}$, in turn linked to the reduced partial widths (γ_α^2), as in [41], through the quantum penetrability $\Gamma_\alpha = 2P_{\ell_f}\gamma_\alpha^2$. A very important consideration is that both the α_0 and the α_2 transitions have zero-channel spin in the exit channel: thus, if a particular ^{16}O state has a given J^π value, the ℓ_f

values linked to the α_0 and the α_2 transitions are fixed and identical. Upon this, the values of $\gamma_{\alpha_0}^2$ and $\gamma_{\alpha_2}^2$ are then proportional to the probability of occurrence, in a given state of the ^{16}O nucleus, of nuclear configurations similar to those of the final states; in the end, the states with values of $\gamma_{\alpha_2}^2 > \gamma_{\alpha_0}^2$ will thus be the most suitable candidates to show a pronounced α -cluster structure. In the framework discussed in this work, the BR is reported as the ratio between the two $\Gamma_{\alpha_i} = 2P_{\ell_f} \gamma_{\alpha_i}^2$, and the penetrability for the two channels ($P_{\ell_f}(\alpha_2)$ and $P_{\ell_f}(\alpha_0)$) can be calculated through the regular and irregular Coulomb functions [26, 41].

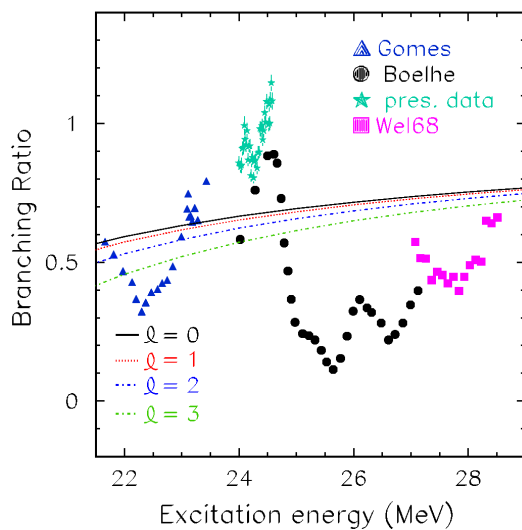


Figure 2. Branching Ratio as a function of the excitation energy for the α_2 channel over the α_0 one. The curves indicate the penetrability ratios computed for both transitions for different values of the angular momentum: upon this, data which lie in the region above the penetrability ratio curves will exhibit a dominance of the Hoyle state configuration with respect to that of the ground state; at variance, all data below the curve will be characterized by a structure more similar to that of the ^{12}C ground state plus an α particle.

In Figure 2, the present experimental BRs are reported as a function of the E_x in the compound nucleus, together with other literature data from previous experimental works [26, 27] on $^{13}\text{C}(^{3}\text{He}, \alpha)^{12}\text{C}$ reactions; as it can be seen from the plot, the BRs obtained in this work are in reasonable agreement with those from [27]. Data coming from other reactions, such as the $^{14}\text{N}(^2\text{H}, \alpha)^{12}\text{C}$, have been collected at lower energies, extrapolated from the ICS data reported in Ref. [43]; this last group of reactions have kinematics and Q -values which are very similar to those of the $^{13}\text{C}(^{3}\text{He}, \alpha_i)^{12}\text{C}$ reactions, thus keeping valid the assumption of low partial waves dominance in the entrance channel. Still, a difference can be present because of the possible contribution coming from the α_0 channel at low energies in the $d+^{14}\text{N}$ collisions, as reported in Refs. [22, 43]; since the presence of the direct effects would enhance the α_0 channel cross section, it is important to note that the data coming from this reaction should be seen as

a *lower limit* of the effective value of the BR for the α_2 to the α_0 channel in ^{16}O excited states.

As seen from Figure 2, the data from the present work are above the trend given by the *penetrability ratio* (calculated as $R = \frac{P_{\ell_f}(\alpha_2)}{P_{\ell_f}(\alpha_0)}$ for $\ell_f = 0, 1, 2, 3$, i.e., four different orbital angular momentum values in the outgoing channels) in the region around $E_x \approx 24.1$ and ≈ 24.5 MeV. This finding would characterize states with $\gamma_{\alpha_2}^2 > \gamma_{\alpha_0}^2$, exhibiting a potential α cluster structure. Other data which clearly exhibit peaks above the penetrability ratio are those from [43], in the region around $E_x \approx 23 - 23.5$ MeV and, in an even more interesting way, all the data at $E_x < 22.5$ MeV, whose increasing trend is worth of considerations for future investigations: in fact, the 0^+ band-heads of some quartet bands in ^{16}O are predicted to exist at $E_x > 23$ MeV [21, 44] and could be related to the two isoscalar states here reported.

5 Conclusions

In this work, the eventual manifestation of α -cluster structures in the ^{16}O nucleus at high excitation energies has been probed through the $^{13}\text{C}(^{3}\text{He}, \alpha)^{12}\text{C}$ reaction at low bombarding energies, performed thanks to a high performance apparatus, composed of an array of several *OSCAR* detectors in the *HELICA* configuration. The experiment has been specifically designed to detect low-energy α particles and identify the various reaction channels leaving the residual ^{12}C nucleus in different excited states. The analysis of the measured angular distributions allowed to reveal the presence of two *low spin and high energy* isoscalar states with suggested $J^\pi = 2^+$ and 3^- assignments, in the $E_x \approx 24$ MeV region.

The measurement of differential cross sections led to the extraction of the integrated cross sections for all channels, even for the very elusive α_2 , in which the residual ^{12}C nucleus is left in its Hoyle state. The behaviour of the branching ratios of the α decay of ^{16}O states, i.e., the ratio of the transition to the ^{12}C Hoyle or ground states, was thus analyzed; the identical spin-parity characteristics of these two states allowed to treat the problem in the framework of a simple barrier penetration model. Anomalously large values of branching ratios have been observed in some E_x regions, suggesting the possible occurrence of α -cluster states in ^{16}O at very high excitation energies and claiming for further investigations.

References

- [1] C. Beck., Lect. Not. Phys. 818 (Springer, 2010)
- [2] M. Freer, H. Horiuchi, Y. Kanada-En'yo, D. Lee, U. Meissner, Rev. Mod. Phys. **90**, 035004 (2018).
- [3] L. Morelli et al., Full disassembly of excited mg 24 into six α particles, Physical Review C **99**, 054610 (2019).
- [4] I. Lombardo, D. Dell'Aquila, Clusters in light nuclei: history and recent developments, La Rivista del Nuovo Cimento pp. 1–98 (2023).

- [5] Y. Kanada-En'yo, D. Lee, Phys. Rev. C **103**, 024318 (2021).
- [6] D. Marin-Lambarri, R. Bijker, M. Freer, M. Gai, T. Kokalova et al., Phys. Rev. Lett. **113**, 012502 (2014).
- [7] D. Dell'Aquila et al., J. Phys.: Conf. Ser. **876**, 012006 (2017).
- [8] R. Smith, T. Kokalova, C. Wheldon, J. Bishop, M. Freer et al., Phys. Rev. Lett. **119**, 132502 (2017).
- [9] T.K. Rana, S. Bhattacharya, C. Bhattacharya, S. Manna, S. Kundu et al., Phys. Lett. B **793**, 130 (2019).
- [10] R. Smith, M. Gai, M. Ahmed, M. Freer, H. Fynbo et al., Phys. Rev. C **101**, 021202(R) (2020).
- [11] T. Otsuka, T. Abe, T. Yoshida, Y. Tsunoda, N. Shimitsu et al., Nature Comm. **13**, 2234 (2022).
- [12] R. Katsuragi, Y. Kazama, J. Takahashi, Y. Nakamura, Y. Yamanaka et al., Phys. Rev. C **98**, 044303 (2018).
- [13] D. Dell'Aquila et al., Scientific Reports **14**, 18958 (2024).
- [14] L. Redigolo et al., Journal of Physics G: Nuclear and Particle Physics **50**, 075101 (2023).
- [15] R. Bijker, F. Iachello, Phys. Rev. Lett. **112**, 152501 (2014).
- [16] N. Furutachi, M. Kimura, Phys. Rev. C **83**, 021303 (2011).
- [17] T. Fukui, Y. Kanada-En'yo, K. Ogata, T. Suhara, Y. Taniguchi, Nucl. Phys. A **983**, 38 (2019).
- [18] Y. Funaki, Alpha condensate and dynamics of cluster formation, European Physical Journal A **57**, 14 (2021).
- [19] C. Halcrow, C. King, N.S. Manton, Phys. Rev. C **95**, 031303(R) (2017).
- [20] D. Tilley, H. Weller, C. Cheves, Nucl. Phys. A **564**, 1 (1993).
- [21] A. Arima, V. Gillet, J. Ginocchio, Phys. Rev. Lett. **25**, 1043 (1970).
- [22] W. Koenig et al., Il Nuov. Cim. **39**, 9 (1977).
- [23] M. Freer, N. Clarke, N. Curtis, B. Fulton, S. Hall et al., Phys. Rev. C **51**, 1682 (1995).
- [24] N. Curtis, S. Almaraz-Calderon, A. Aprahamian, N. Ashwood, M. Barr et al., Phys. Rev. C **94**, 034313 (2016).
- [25] R. Charity, K.W. Brown, J. Elson, W. Reviol, L. Sobotka et al., Phys. Rev. C **99**, 044304 (2019).
- [26] H. Weller, N. Roberson, D. Tilley, Nucl. Phys. A **122**, 529 (1968).
- [27] K. Boehle, V. Meyer, H. Muller, Helv. Phys. Acta **44**, 367 (1971).
- [28] D. Dell'Aquila, I. Lombardo, G. Verde, M. Vigilante, G. Ausanio et al., Nucl. Instr. Meth. Phys. Res. A **877**, 227 (2018).
- [29] I. Lombardo, D. Dell'Aquila, M. Cinausero, L. Gasques, M. Vigilante et al., J. Phys. G.: Nucl. Part. Phys. **48**, 065101 (2021).
- [30] D. Dell'Aquila et al., in *2022 IEEE (NSS/MIC)* (IEEE, 2022), pp. 1–4
- [31] I. Lombardo et al., in *EPJ Web of Conferences* (EDP Sciences, 2024), Vol. 292, p. 07001
- [32] H.D. Holmgren, Phys. Rev. **106**, 100 (1957).
- [33] H. Holmgren, E.H. Geer, R. Johnston, E. Wolicki, Phys. Rev. **106**, 102 (1957).
- [34] M.A. Eswaran, S. Kumar, E.T. Mirgule, Phys. Rev. C **42**, 1036 (1990).
- [35] A. Isoya, H. Ohmura, T. Momota, The angular distributions of the long-range alpha-particles from the reaction $f\,19\,(p, \alpha\,0)\,o\,16$, Nuclear Physics **7**, 116 (1958).
- [36] I. Lombardo, D. Dell'Aquila, L. Campajola, E. Rosato, G. Spadaccini et al., J. Phys. G: Nucl. Part. Phys. **40**, 1251102 (2013).
- [37] I. Lombardo, D. Dell'Aquila, A.D. Leva, I. Indelicato, M.L. Cognata et al., Phys. Lett. B **748**, 178 (2015).
- [38] L. Redigolo et al., Journal of Physics G: Nuclear and Particle Physics **51**, 075106 (2024).
- [39] E. Eisner, R.G. Sachs, Phys. Rev. **72**, 680 (1947).
- [40] C.N. Yang, Phys. Rev. **74**, 764 (1948).
- [41] J.M. Blatt, L.C. Biedenharn, Rev. Mod. Phys. **24**, 258 (1952).
- [42] R.G. Sachs, Nuclear Theory (Addison-Wesley, 1953)
- [43] V. Gomes-Porto, N. Ueta, R. Douglas, O. Sala, D. Wilmore et al., Nucl. Phys. A **136**, 385 (1969).
- [44] L. Satpathy, K. Schmid, A. Faessler, Phys. Rev. Lett. **28**, 832 (1972).